

$T = 2$ and $T = 3$ Analog States, $28 \leq A \leq 40^*$ J. C. HARDY, H. BRUNNADER,[†] AND JOSEPH CERNY*Lawrence Radiation Laboratory and Department of Chemistry, University of California, Berkeley, California 94720*

(Received 28 July 1969)

The simultaneous observation of (p, t) and $(p, {}^3\text{He})$ reactions has led to the location and identification of the lowest-energy (0^+) $T=2$ states in ${}^{28}\text{Al}$, ${}^{28}\text{Si}$, ${}^{32}\text{P}$, ${}^{32}\text{S}$, ${}^{36}\text{Cl}$, ${}^{36}\text{Ar}$, ${}^{40}\text{K}$, and ${}^{40}\text{Ca}$, as well as the (0^+) $T=3$ states in ${}^{38}\text{Cl}$ and ${}^{38}\text{Ar}$. The energies of these states are used to predict the masses of six neutron-deficient nuclei: ${}^{28}\text{S}$, ${}^{32}\text{Ar}$, ${}^{36}\text{Ca}$, ${}^{38}\text{Sc}$, ${}^{38}\text{Ti}$, and ${}^{40}\text{Ti}$. In addition, the (p, t) cross section for production of each analog state relative to the cross section for producing the ground state in the same nucleus is compared with calculations which assume a simple shell model. Good agreement is obtained.

I. INTRODUCTION

THE advent of new experimental techniques for measuring the masses of neutron-deficient nuclei has led to recent interest in investigating the limits of stability in the lighter nuclides. As an aid to such measurements, accurate mass predictions are of great value, and for this purpose the isobaric-multiplet mass equation (IMME) is frequently used:

$$M(A, T, T_z) = a(A, T) + b(A, T)T_z + c(A, T)T_z^2. \quad (1)$$

This equation has the advantage that it is easy to apply and is apparently reliable¹—the coefficient of the next higher-order term being almost two orders of magnitude smaller² than the coefficient c . However, use of the equation for predicting the mass of a particular state requires knowledge of the masses of three other members of the same multiplet, since the coefficients a , b , and c must be experimentally determined for each value of A and T . The masses of all $T_z = +2$ ($A = 4n$) nuclei are known to better than ± 10 keV in the region $28 \leq A \leq 40$ and, consequently, for each value of A , measurement of the excitation energies of $T=2$ analog states in two other isobars permits use of the IMME for relatively accurate predictions of other members of the multiplet. Similarly, the measurement of two $T=3$ states in mass 38 combined with the less accurately known mass (± 150 keV) of ${}^{38}\text{S}$ yields rough predictions for that multiplet.

We report here the location and identification of the lowest-energy (0^+) $T=2$ states in ${}^{28}\text{Al}$, ${}^{28}\text{Si}$, ${}^{32}\text{P}$, ${}^{32}\text{S}$, ${}^{36}\text{Cl}$, ${}^{36}\text{Ar}$, ${}^{40}\text{K}$, and ${}^{40}\text{Ca}$, as well as the $T=3$ states in ${}^{38}\text{Cl}$ and ${}^{38}\text{Ar}$. The method used was to simultaneously observe the (p, t) and $(p, {}^3\text{He})$ reactions. If the target nucleus has isospin T_i and the reactions produce analog final states with $T_f = T_i + 1$, then their

angular distributions will have the same shape and the ratio of their differential cross sections will be given by

$$R \equiv \frac{d\sigma/d\Omega(p, t)}{d\sigma/d\Omega(p, {}^3\text{He})} = \frac{k_t}{k_{{}^3\text{He}}} \frac{2}{2T_f - 1}. \quad (2)$$

The approximations leading to the derivation of Eq. (2) have recently been discussed within the framework of the distorted-wave Born approximation, and the equation's validity has been established for light nuclei ($14 \leq A \leq 40$, $T_f \leq 3$) by comparison with experimental data.³ The properties embodied in the equation provide an unambiguous experimental method for identifying high-isospin analog states.

Using the experimental data, masses are predicted with the IMME for ${}^{28}\text{S}$, ${}^{32}\text{Ar}$, ${}^{36}\text{Ca}$, ${}^{38}\text{Sc}$, ${}^{38}\text{Ti}$, and ${}^{40}\text{Ti}$. These results are compared with those obtained by Kelson and Garvey.⁴ In addition, the relative intensities of the analog-state transitions are compared with calculations which assume simple shell-model configurations.

II. EXPERIMENTAL PROCEDURE

This series of measurements was carried out using the 45-MeV proton beam from the Berkeley 88-in. cyclotron. The beam was magnetically analyzed to give an energy resolution of $\sim 0.14\%$, and was focused to a spot $2 \text{ mm} \times 1.5 \text{ mm}$ at the target position in the center of a 50-cm scattering chamber. The exact position and direction of the beam was determined by observing luminous foils located at the target position and 70 cm downstream. The beam current ranged from 50 nA to $1.0 \mu\text{A}$, depending on target thickness and scattering angle; it was monitored with a Faraday cup connected to an integrating electrometer. The beam energy was inferred from measuring its range in a series of aluminum foils which were contained in five remotely controlled wheels.

A detailed diagram of the scattering chamber, gas

* Work performed under the auspices of the U.S. Atomic Energy Commission.

[†] Present address: Department of Chemistry, McMaster University, Hamilton, Ontario, Canada.

¹ J. Cerny, *Ann. Rev. Nucl. Sci.* **18**, 27 (1968).

² J. Jänecke, *Nucl. Phys.* **A128**, 632 (1969); G. T. Garvey, in *Nuclear Isospin*, edited by J. D. Anderson, S. D. Bloom, J. Cerny, and W. W. True (Academic Press Inc., New York, 1969), p. 703.

³ J. C. Hardy, H. Brunnader, and J. Cerny, *Phys. Rev. Letters* **22**, 1439 (1969).

⁴ I. Kelson and G. T. Garvey, *Phys. Letters* **23**, 689 (1966).

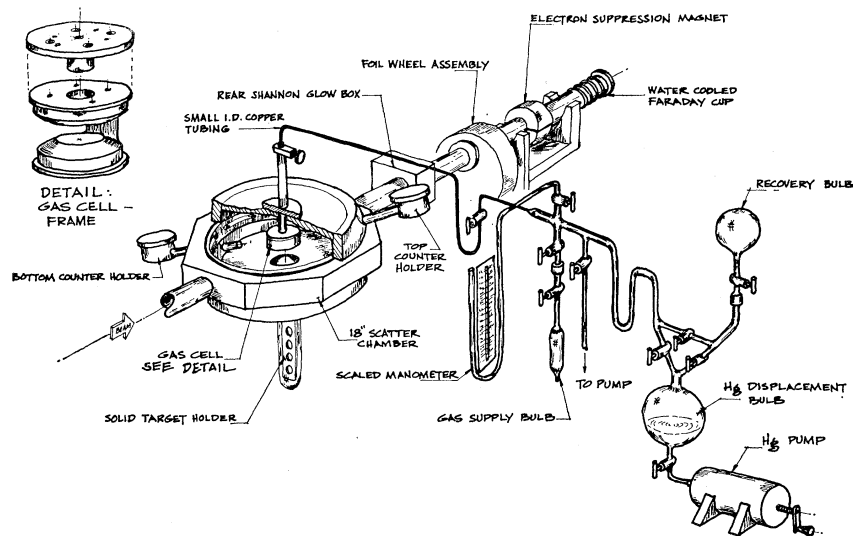


FIG. 1. Diagram of the scattering chamber, gas target, and gas handling apparatus.

target, and gas-handling apparatus is shown in Fig. 1. The gas cell consisted of a stainless steel cylindrical frame 6.35 cm in diameter and 2.22 cm high surrounded by a 315° continuous window of 2.5- μ Havar foil.⁵ An expanded view of the frame is shown in the insert to the figure. The gas cell was designed for minimum volume (47 cm³) in order to permit the efficient recovery of separated-isotope gases. To use solid targets, the gas cell was removed and a set of targets was mounted in a holder which could then be raised and lowered remotely, thus permitting bombardment of any selected target.

Reaction products were detected using two independent counter telescopes mounted 10° out of the horizontal plane on opposite sides of the beam. The solid angle subtended by each telescope was $\sim 5 \times 10^{-5}$ sr, with an angular resolution of 0.26°. For solid targets, a tantalum collimator 5 mm high by 2 mm wide was mounted 48 cm from the target, while for gas targets an additional collimator with the same width as the first was mounted 36 cm ahead of it. Each telescope consisted of three detectors, a 150- μ phosphorus-diffused silicon transmission counter (ΔE) operated in coincidence with a 3-mm lithium-drifted silicon E counter, and a 500- μ lithium-drifted silicon E -reject counter operated in anticoincidence with the first two to eliminate long-range protons and deuterons.

A schematic diagram of the electronics used is shown in Fig. 2. The signals from each telescope were fed into a Goulding-Landis particle identifier⁶ which produced an output signal characteristic of the particle

type. This signal was used to route the total-energy signal ($E + \Delta E$) into one of the 1024-channel segments of a 4096-channel analyzer, permitting simultaneous accumulation of α particles, ^3He particles, tritons, and those particles slightly less ionizing than the selected tritons. The first and last groups were taken to check that no ^3He or triton events were lost. The over-all

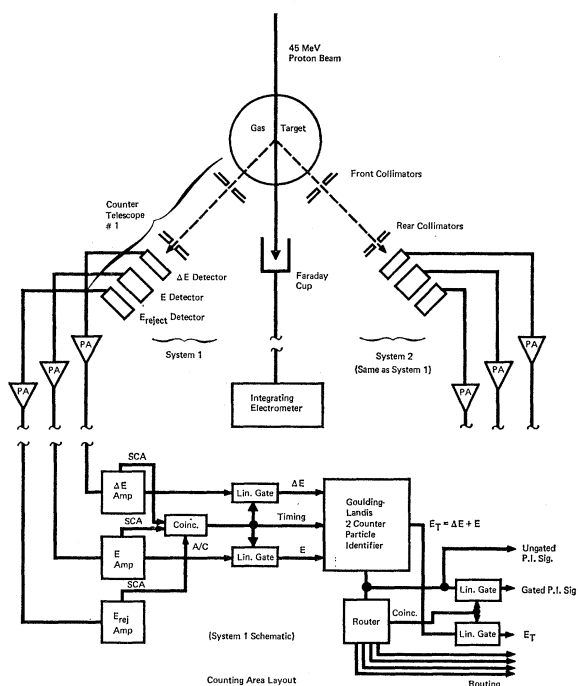


FIG. 2. Schematic diagram of the electronic apparatus used in conjunction with the counter telescopes: Only system 1 is shown in its entirety, system 2 being similar.

⁵ Havar foil is manufactured by the Metals Division, Hamilton Watch Company, Lancaster, Pa.

⁶ F. S. Goulding, D. A. Landis, J. Cerny, and R. H. Pehl, Nucl. Instr. Methods **31**, 1 (1964).

TABLE I. Optical-model parameters^a used in DWBA calculations.

Particle	V_0	W_0	W_D	V_s	r_0	r_0'	r_s	a	a'	a_s	Ref.
Proton	45.0	5.7	1.8	6.04	1.16	1.37	1.064	0.75	0.63	0.738	b
Triton+ ²⁸ Si	147.1	54.1	1.40	1.40	...	0.61	0.61	...	c
Triton+ ³⁶ Ar, ³⁸ Ar	143.3	53.3	1.40	1.40	...	0.59	0.59	...	c

^a The form of the potential and the notation followed in this table are identical to those used in Ref. 11.

^b Reference 11.

^c Reference 12.

resolution (full width at half-maximum) was ~ 100 keV for tritons and ~ 130 keV for ³He particles.

III. EXPERIMENTAL RESULTS

The excitation energies of observed states were determined by analyzing the data with the computer program LORNA.⁷ This program corrects the energies of incoming and outgoing particles for kinematic effects and absorber losses, then determines the energies of unknown peaks using an energy scale established from a least-squares fit to peaks whose Q values are known. For the experiments described here, contaminants were

already present or introduced in the targets to provide calibration. The most useful calibration reactions were ¹²C(p, t)¹⁰C and ¹²C($p, ^3$ He)¹⁰B: The masses of the ¹⁰C ground and first excited states were taken from recent measurements,⁸ while values for the levels of ¹⁰B were taken from Ajzenberg-Selove and Lauritzen.⁹ The errors assigned to the measurements reported here are based upon a statistical analysis of their consistency in determinations at various laboratory angles, together with an estimate of systematic errors such as those arising from inaccuracies in establishing the scattering angle.

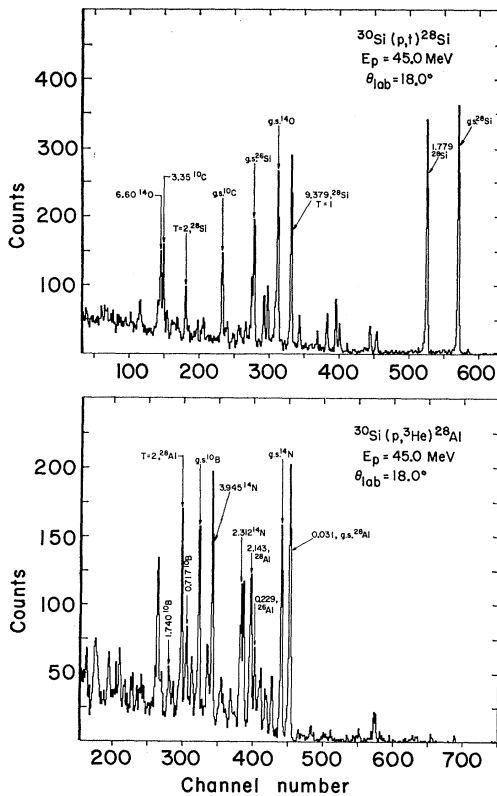


FIG. 3. Energy spectra of the reactions ³⁰Si(p, t)²⁸Si and ³⁰Si($p, ^3$ He)²⁸Al.

⁷ The program LORNA was written by C. C. Maples to whom we are grateful for making it available.

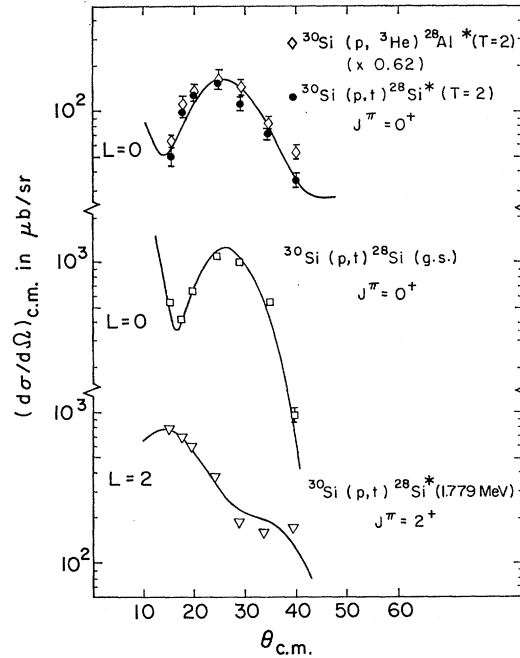


FIG. 4. Angular distributions for the reactions ³⁰Si(p, t)²⁸Si and ³⁰Si($p, ^3$ He)²⁸Al leading to selected final states. Note that the ($p, ^3$ He) data for the $T=2$ state has been multiplied by 0.62 as suggested by Eq. (2). The solid curves correspond to DWBA calculations for $L=0$ and $L=2$ transfer using the parameters given in Table I.

⁸ H. Brunnader, J. C. Hardy, and J. Cerny, Phys. Rev. **174**, 1247 (1968); R. A. Paddock, S. M. Austin, W. Benenson, I. D. Proctor, and F. St. Amert, Phys. Rev. **182**, 1104 (1969).

⁹ F. Ajzenberg-Selove and T. Lauritzen, Nucl. Phys. **A114**, 1 (1968).

TABLE II. Summary of experimental results for high- T states.

Nucleus	Analog state $J^\pi; T$	Excitation energy		Average (MeV \pm keV)
		This work (MeV \pm keV)	Other work (MeV \pm keV)	
^{28}Al	$0^+; 2$	5.983 ± 25	...	$[5.983\pm 25]$
^{28}Si	$0^+; 2$	15.206 ± 25	15.221 ± 5^a	15.221 ± 5
^{32}P	$0^+; 2$	5.071 ± 40	...	$[5.071\pm 40]$
^{32}S	$0^+; 2$	12.034 ± 40	11.984 ± 4^b	11.984 ± 4
^{36}Cl	$0^+; 2$	4.295 ± 30	4.333 ± 25^c	4.316 ± 19
^{36}Ar	$0^+; 2$	10.858 ± 35	...	$[10.858\pm 35]$
^{38}Cl	$0^+; 3$	8.216 ± 25	...	$[8.216\pm 25]$
^{38}Ar	$0^+; 3$	18.784 ± 30	...	$[18.784\pm 30]$
^{40}K	$0^+; 2$	4.375 ± 25	4.370 ± 70^d	4.374 ± 24
^{40}Ca	$0^+; 2$	11.978 ± 25	11.970 ± 65^d	11.977 ± 23

^a References 14–17.^b Reference 19.^c Reference 22.^d Reference 1.

A. $^{30}\text{Si}(p,t)^{28}\text{Si}$ and $^{30}\text{Si}(p,^3\text{He})^{28}\text{Al}$, $T=2$ States

Triton and ^3He spectra from a $400\text{-}\mu\text{g}/\text{cm}^2$ self-supporting silicon target are shown in Fig. 3; they were obtained at $\theta_{\text{lab}}=18.0^\circ$ for $2150\text{ }\mu\text{C}$. The isotopic enrichment of the target was 89.12% in ^{30}Si with 10.16% ^{28}Si and 0.72% ^{29}Si . Spectra were recorded for seven angles ranging from $\theta_{\text{lab}}=14.1^\circ$ to $\theta_{\text{lab}}=36.2^\circ$.

The energy scale was determined using peaks produced from reactions on ^{12}C , ^{16}O , and ^{28}Si as well as those known states produced in ^{28}Si and ^{28}Al ; all have been indicated in the figure. Rough Coulomb-energy calculations predict the excitation energy of the lowest-energy $T=2$ state to be 15.3 MeV in ^{28}Si and 6.1 MeV in ^{28}Al . The states marked $T=2$ in Fig. 3 are consistent with these expectations, and the angular distribution of the corresponding tritons and ^3He particles are shown at the top of the Fig. 4. The ^3He data points have been multiplied by $\frac{2}{3}k_t/k_{^3\text{He}}$ ($=0.62$) so that the applicability of Eq. (2) can be tested directly. To the accuracy of the approximations used to derive that equation, the shapes and magnitudes of the distributions as they appear in the figure are the same, and consequently the levels are established as $T=2$ analogs. Also shown in Fig. 4 are the characteristic $L=0$ and $L=2$ angular distributions of the (p, t) reaction leading to the ground (0^+) and first excited (2^+) state of ^{28}Si . A simple comparison shows that the angular momentum transfer to the analog states is also $L=0$, and this identifies them as the 0^+ analogs of the ^{28}Mg ground state.

Further verification of the assigned L transfer was provided by calculations using the distorted-wave Born approximation (DWBA). The calculations were performed using the program DWUCK¹⁰ with the op-

tical-model parameters^{11,12} given in Table I, and the results are shown normalized to the experimental data in Fig. 4. The agreement is good.

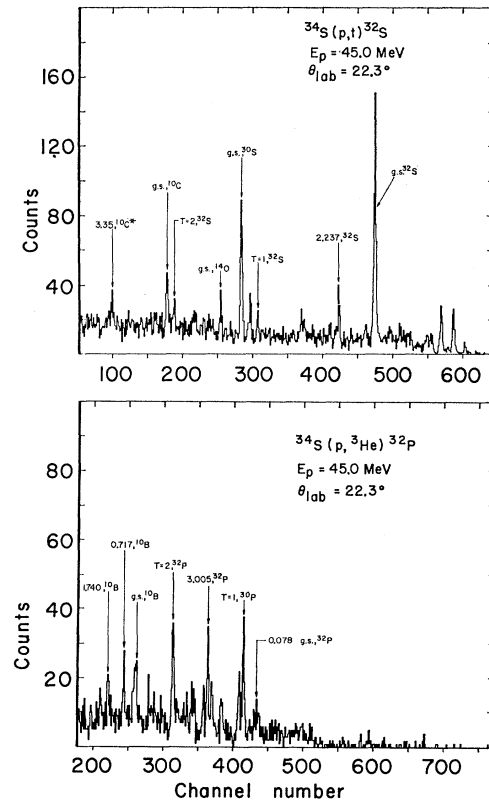


Fig. 5. Energy spectra of the reactions $^{34}\text{S}(p, t)^{32}\text{S}$ and $^{34}\text{S}(p, ^3\text{He})^{32}\text{P}$.

¹⁰ The program DWUCK was written by D. Kuntz, and modified for two-nucleon transfer reactions following the "zero-range interaction" approximation [see N. K. Glendenning, Phys. Rev. **137**, B102 (1965)] by us.

¹¹ Average parameters taken from fits to 40-MeV elastic proton scattering by M. P. Fricke, E. E. Gross, B. J. Morton, and A. Zucker, Phys. Rev. **156**, 1207 (1967).

¹² R. N. Glover and A. D. W. Jones, Nucl. Phys. **81**, 268 (1966).

A summary of results on these mass-28 analog states is shown in Table II. We have previously reported our measured excitation energies in a letter¹³ devoted to the decay of the $T=2$ state in ^{28}Si . Subsequently, by searching in the indicated energy region, the analog state in ^{28}Si was observed as a resonance in the $^{24}\text{Mg}(\alpha, \alpha)^{24}\text{Mg}$ reaction^{14,15} and the $^{24}\text{Mg}(\alpha, \gamma)^{28}\text{Si}^*$ reaction^{14,16} and also as a final state in the $^{26}\text{Mg}(^3\text{He}, n)^{28}\text{Si}$ reaction.¹⁷ The best value from these other measurements¹⁸ is also shown in Table II. It agrees well with our original value.

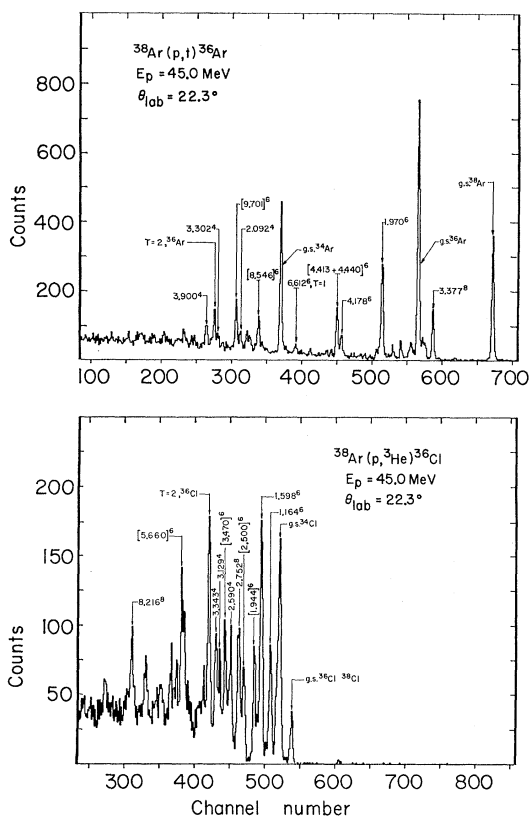


FIG. 6. Energy spectra of the reactions $^{38}\text{Ar}(p, t)^{36}\text{Ar}$ and $^{38}\text{Ar}(p, ^3\text{He})^{36}\text{Cl}$. The excitations shown bracketed were determined in this work, the calibration having been established from the other marked states.

¹³ R. L. McGrath, J. C. Hardy, and J. Cerny, Phys. Letters **27B**, 443 (1968).

¹⁴ K. A. Snover, D. W. Heikkinen, F. Riess, H. M. Kuan, and S. S. Hanna, Phys. Rev. Letters **22**, 239 (1969).

¹⁵ G. H. Lentz, M. P. Etten, and D. Wilkins, Bull. Am. Phys. Soc. **14**, 548 (1969). This replaces an earlier erroneous report by G. H. Lentz and D. Bernard, *ibid.* **13**, 673 (1968).

¹⁶ T. T. Thwaites, P. Kupferman, and S. Slack, Bull. Am. Phys. Soc. **14**, 566 (1969).

¹⁷ W. Bohne, H. Fuchs, K. Grabisch, M. Hagen, H. Homeyer, U. Janetzki, H. Lettau, K. H. Maier, H. Morgenstern, P. Pietrzki, G. Röscher, and J. A. Scheer (to be published).

¹⁸ The actual excitation energies measured (in MeV) are 15.221 ± 0.005 (Ref. 15), 15.196 ± 0.010 (Ref. 16), 15.216 (Ref. 17) (no quoted error, but presumably less than ± 0.010), and 15.27 ± 0.05 (Ref. 18). With the exception of the second, these values are consistent with one another. The result in Ref. 15 is the one quoted in Table II since it is the most accurate and the only one which has actually been published.

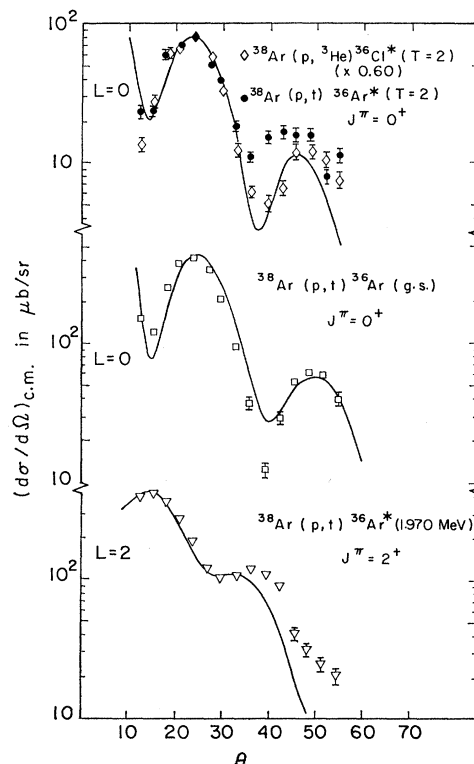


FIG. 7. Angular distributions of the reaction $^{38}\text{Ar}(p, t)^{36}\text{Ar}$ and $^{38}\text{Ar}(p, ^3\text{He})^{36}\text{Cl}$ leading to selected final states. The $(p, ^3\text{He})$ data for the $T=2$ state has been multiplied by 0.60 as suggested by Eq. (2). The solid curves correspond to DWBA calculations for $L=0$ and $L=2$ transfer using the parameters given in Table I.

B. $^{34}\text{S}(p, t)^{32}\text{S}$ and $^{34}\text{S}(p, ^3\text{He})^{32}\text{P}, T=2$ States

A self-supporting cadmium sulfide target approximately $100 \mu\text{g}/\text{cm}^2$ thick was used for this experiment. The sulfur component was enriched to 67.92% in ^{34}S with 31.55% ^{32}S , 0.44% ^{33}S , and 0.09% ^{36}S . Because the thin target could only withstand small beam intensities, the counting rates were low and consequently spectra were recorded at only four angles ranging from $\theta_{\text{lab}} = 20.5^\circ$ to $\theta_{\text{lab}} = 31.5^\circ$. Triton and ^3He spectra obtained at $\theta_{\text{lab}} = 22.3$ for $6380 \mu\text{C}$ are shown in Fig. 5. A natural cadmium sulfide target was also bombarded and spectra taken at the same angle in order to identify those states in ^{30}S and ^{30}P which were produced from the enriched target. These states have been marked in the figure and were used, together with the other marked states, to establish the energy calibration.

The states identified in the figure as being $T=2$ are at excitation energies consistent with predictions based on Coulomb energy calculations, and the ratio of differential cross sections for the reactions populating these states has an average value for the four observed angles of 0.66 ± 0.06 . This agrees well with the value of 0.60 calculated from Eq. (2), thus establishing the $T=2$ character of the states. In addition,

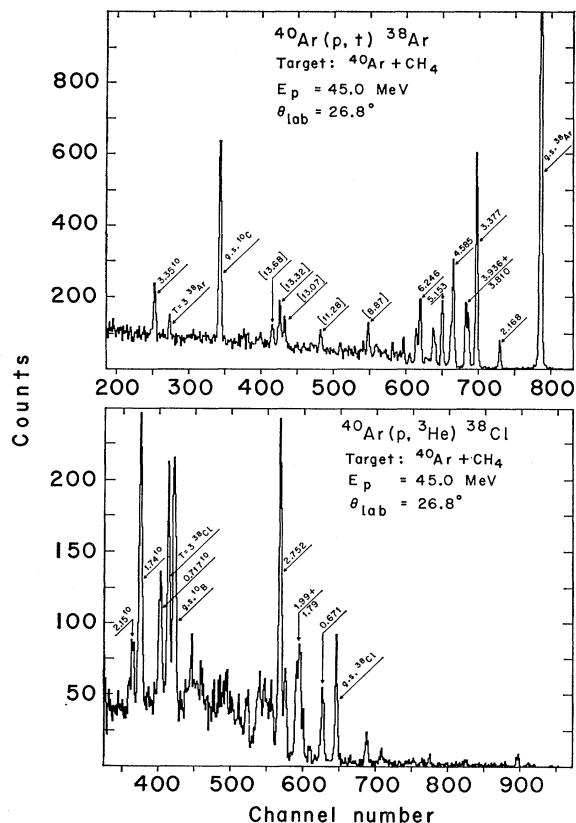


FIG. 8. Energy spectra of the reactions $^{40}\text{Ar}(p,t)^{38}\text{Ar}$ and $^{40}\text{Ar}(p,^3\text{He})^{38}\text{Cl}$. The states shown bracketed were determined in this work, the calibration having been established using the other marked states.

their energy and the fact that their observed angular distributions are consistent with $L=0$ transfer identify the states as 0^+ analogs to the ground state of ^{32}Si .

These results are summarized in Table II. The excitation energies shown there have appeared prior to this publication in a review article¹ and, as with mass 28, the energy of the lowest-energy $T=2$ state in ^{32}S was subsequently remeasured using a resonance reaction¹⁹; this result also appears in the table.

C. $^{38}\text{Ar}(p,t)^{36}\text{Ar}$ and $^{38}\text{Ar}(p,^3\text{He})^{36}\text{Cl}$, $T=2$ States

Spectra of tritons and ^3He particles from an ^{38}Ar -enriched target are shown in Fig. 6; they were recorded at 22.3° for 7562 μC . The isotopic composition of the gas target was 23.3% ^{36}Ar , 50.8% ^{38}Ar , and 25.9% ^{40}Ar . Altogether, spectra were obtained for fifteen angles from $\theta_{\text{lab}}=11.7^\circ$ to $\theta_{\text{lab}}=50.7^\circ$.

Under identical running conditions, ^{36}Ar and ^{40}Ar targets were bombarded in order to identify peaks

produced from these isotopes. Following this identification, the energy calibration of the original spectra could be accomplished by means of known states in mass 34,^{20,21} mass 36, and mass 38²¹; all have been marked with their excitation energy (unbracketed) and isotopic mass in the figure. The states labeled $T=2$ have measured energies which agree with rough Coulomb-energy predictions for the analog states, and their corresponding triton and ^3He angular distributions are shown at the top of Fig. 7. The similarity of the shapes and magnitudes of the distributions as they appear in the figure show that the conditions of Eq. (2) are satisfied, and identifies the states as $T=2$ analogs. By comparison with known $L=0$ and $L=2$ transitions (also shown in Fig. 7) and with DWBA calculations (solid curves in the figure) the angular-momentum transfer for transitions to these analog states is determined to be $L=0$. Thus, the states must be the 0^+ analogs to the ground state of ^{36}S . Their measured energies are listed in Table II. There has

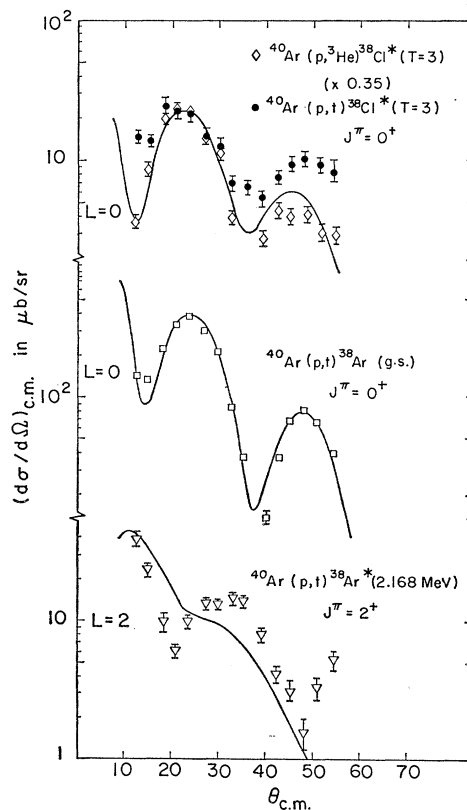


FIG. 9. Angular distributions of the reactions $^{40}\text{Ar}(p,t)^{38}\text{Ar}$ and $^{40}\text{Ar}(p,^3\text{He})^{38}\text{Cl}$ leading to selected final states. The $(p,^3\text{He})$ data has been multiplied by 0.350 as suggested by Eq. (2). The solid curves correspond to DWBA calculations for $L=0$ and $L=2$ transfer using the parameters given in Table I.

¹⁹ D. W. Heikkinen, H. M. Kuan, K. A. Snover, F. Riess, and S. S. Hanna, Bull. Am. Phys. Soc. **13**, 884 (1968); although the 11,984-MeV state is the only observed resonance in the energy region of the $T=2$ state, its identification from observed γ rays is not conclusive (private communication from D. W. Heikkinen).

²⁰ H. Brunnader, J. C. Hardy, and J. Cerny, Nucl. Phys. **A137**, 487 (1969).

²¹ P. M. Endt and C. van der Leun, Nucl. Phys. **A105**, 1 (1967).

been a recent measurement²² of a state in ³⁶Cl proposed as the $J^\pi=0^+$; $T=2$ analog state. It is listed in Table II and agrees with our value.

D. ⁴⁰Ar(p,t)³⁸Ar and ⁴⁰Ar($p,^3$ He)³⁸Cl; $T=3$ States

Pure natural argon, which is 99.6% ⁴⁰Ar, was used to obtain triton and ³He angular-distribution data, while energy calibration resulted from the use of an argon-methane (80-20%, respectively) mixture. In Fig. 8 are shown sample spectra taken, using the latter target, at 26.8° for 12 553 μ C. In all, spectra were recorded at fifteen angles between $\theta_{lab}=11.7^\circ$ and $\theta_{lab}=50.7^\circ$.

As in the cases already described, the states labeled $T=3$ in Fig. 8 have appropriate excitation energies. Their points have been multiplied by $\frac{2}{3}kt/k^3_{He}$ ($=0.35$). Evidently the requirements of Eq. (2) are satisfied and the states are identified as $T=3$ analogs. It should be pointed out that the error bars which appear on the data points in Fig. 9, like those in other figures, are based purely on counting statistics and do not take account of the uncertainties in background subtraction. In this case these uncertainties are not neg-

TABLE III. Experimental and calculated relative cross sections $[d\sigma/d\Omega(p,t)]/[d\sigma/d\Omega(p,^3He)]$ for states with $T_f=T_i+1$.

	States (MeV)	$J^\pi; T$	R (expt)	R (calc)
²⁸ Si	15.221	$0^+; 2$	0.54 ± 0.10	0.60
²⁸ Al	5.983			
³² S	11.984	$0^+; 2$	0.66 ± 0.06	0.60
³² P	5.071			
³⁶ Ar	10.858	$0^+; 2$	0.62 ± 0.07	0.60
³⁶ Cl	4.316			
³⁸ Ar	18.784	$0^+; 3$	0.36 ± 0.04	0.35
³⁸ Cl	8.216			
⁴⁰ Ca	11.977	$0^+; 2$	0.60 ± 0.05	0.60
⁴⁰ K	4.374			

ligible for the (p, t) reaction and probably account for the discrepancies between (p, t) and ($p, ^3He$) distributions near 45°.

The comparison with known transitions and DWBA calculations afforded by Fig. 9 determine the $T=3$ states to be 0^+ , and establish them as analogs to the ³⁸S ground state. Their measured energies are listed in Table II.

E. ⁴²Ca(p,t)⁴⁰Ca and ⁴²Ca($p,^3$ He)⁴⁰K; $T=2$ States

Since the lowest-energy $T=2$ states have already been identified¹ in ⁴⁰Ca and ⁴⁰K, no attempt was made here to obtain detailed angular distributions; our purpose was to reduce the uncertainty of the measured excitation energies. The calcium target used was enriched to 94.42% ⁴²Ca with 4.96% ⁴⁰Ca, 0.06% ⁴³Ca, 0.56% ⁴⁴Ca, and only trace amounts of ⁴⁶Ca and ⁴⁸Ca. A series of four angles from $\theta_{lab}=18.0^\circ$ to $\theta_{lab}=31.5^\circ$ was measured, the pair of spectra obtained at $\theta_{lab}=26.8^\circ$ for 3554 μ C being shown in Fig. 10.

The excitation energies of the analog states were determined from an energy scale established by the states labeled in the figure. Their angular distributions are consistent with zero angular-momentum transfer and the ratio of their magnitudes agrees with the requirements of Eq. (2). The states are thus confirmed as being 0^+ analogs to the ground state of ⁴⁰Ar. Their measured excitation energies appear in Table II.

IV. DISCUSSION

Table III summarizes the data obtained from these experiments on the cross-section ratios for the production of analog states which have $T_f=T_i+1$. The third column contains the experimental data for $[d\sigma/d\Omega(p,t)]/[d\sigma/d\Omega(p,^3He)]$, while the fourth column gives the results of calculations using Eq. (2); in all cases, agreement is within the limits of experi-

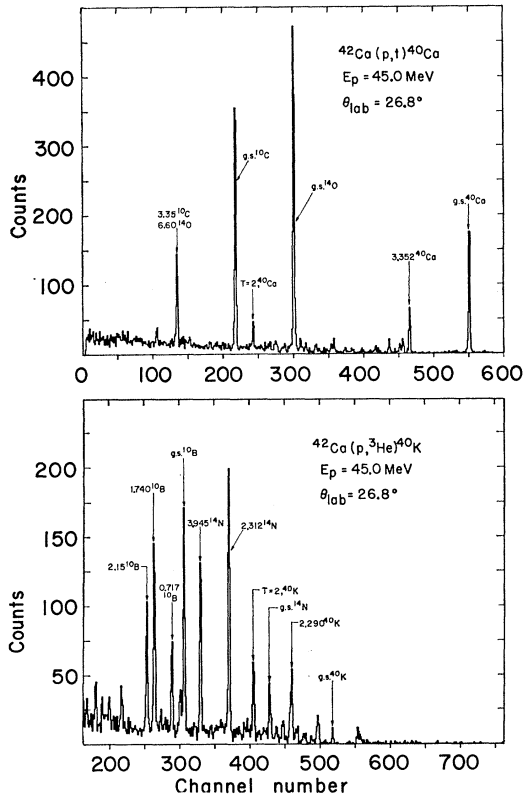


FIG. 10. Energy spectra of the reactions ⁴²Ca(p, t)⁴⁰Ca and ⁴²Ca($p, ^3$ He)⁴⁰K.

²² L. Broman, C. M. Fou, and B. Rosner, Nucl. Phys. A112, 195 (1968).

TABLE IV. Experimental and calculated ratios for the production of the $T_z = |T_z| + 2$ analog state relative to the $T_z = |T_z|$ ground state for several (p, t) reactions.

Reaction	Assumed analog-state configuration	$[d\sigma/d\Omega(T_>)]/[d\sigma/d\Omega(T_<)]$	
		Calculated ^a	Experimental
$^{30}\text{Si}(p, t)^{28}\text{Si}$	$[(1d_{5/2})_{01}^{-2}(2s_{1/2})_{01}^2]_{02}$	0.15–0.45	0.15±0.02
$^{34}\text{S}(p, t)^{32}\text{S}$	$[(2s_{1/2})_{01}^{-2}(1d_{3/2})_{01}^2]_{02}$	0.65–2.0	0.19±0.04
	$[(1d_{5/2})_{01}^{-2}(1d_{3/2})_{01}^2]_{02}$	0.21–1.0	
$^{38}\text{Ar}(p, t)^{36}\text{Ar}$	$(1d_{3/2})_{02}^4$	0.13–0.40	0.19±0.02
$^{40}\text{Ar}(p, t)^{38}\text{Ar}$	$[(1d_{3/2})_{02}^{-4}(1f_{7/2})_{01}^2]_{03}$	0.65–0.15	0.07±0.02
$^{42}\text{Ca}(p, t)^{40}\text{Ca}$	$[(1d_{3/2})_{01}^{-2}(1f_{7/2})_{01}^2]_{02}$	0.13–0.30	0.18±0.03

^a For each reaction, a range of values is shown encompassing the results of DWBA calculations with a variety of plausible optical-model triton

parameters (Refs. 12, 23, and 24) (see discussion in text).

mental uncertainty. The recent discussion² of the validity of Eq. (2) includes these and other results covering the range $16 \leq A \leq 42$ and $1 \leq T_z \leq 3$. The agreement with calculation is uniformly excellent.

It is also of interest to investigate the strength of the (p, t) reaction leading to a particular analog state (with $T_z = |T_z| + 2$) compared to the strength of the reaction to another state in the same final nucleus; for simplicity we have chosen the ground state (which has $T_z = |T_z|$). The comparison between the experimental results and calculations which assume simple shell-model configurations is given in Table IV. In addition to the configurations which are listed in the table for the analog states, the calculations assumed the simplest possible configurations for the ground state of the targets and final nuclei; for example, the ground state of ^{30}Si is assumed to be $(2s_{1/2})_{01}^2$ while that of ^{40}Ar is $[(1d_{3/2})_{01}^{-2}(1f_{7/2})_{01}^2]_{02}$.

It must be emphasized that, unlike the results in Table III, the present calculations will depend considerably upon details of the DWBA computations since the Q values are significantly different for the two final states produced from each target. Unfortunately, optical-model parameters are not available for tritons at our experimental energies ($19 \leq E_t \leq 39$ MeV). The triton parameters listed in Table I were obtained from elastic scattering at 12 MeV, and although they provide reasonable fits to our experimental data (Figs. 4, 7, and 9), there is no guarantee that they will also provide reliable values for the calculated cross-section ratios. Consequently, several parameter sets were used in the calculations for Table IV. These included, in addition to the sets in Table I, parameters obtained from a reanalysis of the same 12-MeV elastic scattering data²³ and also a set which attempted to take account of the dependence of V and W upon the triton energy.²⁴ Each provided adequate agreement with the shapes of the experimental angular distributions, but the calculated cross-section ratios depended significantly upon the set being used. The ranges of

values obtained for each reaction are listed in the third column of Table IV.²⁵ Good agreement is found between experiment and theory with the possible exception of the reaction $^{34}\text{S}(p, t)^{32}\text{S}$. For this case, the most probable simple configuration for the analog state requires $(2s_{1/2})^2$ pickup to that state, but $(1d_{3/2})^2$ to the ground state. Here, the disagreement with experiment indicates that the transfer involves more complex configurations possibly including $(1d_{5/2})^2$ pickup to the analog state.

Obviously, the simple configurations assumed here for the wave functions of all the states involved are unrealistic; however, the good over-all agreement in Table IV cannot be ignored since the (p, t) reaction is generally very sensitive to details of the assumed wave functions. In addition, three more cases of similar agreement are known^{1,26} and together with the present data they span the region $20 \leq A \leq 52$. Presumably, these results reflect the fact that the par-

TABLE V. Predicted mass excesses of unmeasured neutron-deficient nuclei.

Nucleus	T_z	Estimated mass from IMME (MeV±keV)	Kelson-Garvey ^a mass predictions (MeV)
^{28}S	–2	4.31±200	4.44
^{32}Ar	–2	–2.59±320	–2.28
^{36}Ca	–2	–6.58±210	–6.48
^{38}Sc	–2	–4.55±1020 ^b	–4.70
^{38}Ti	–3	11.08±1680	10.82
^{40}Ti	–2	–9.07±265	–9.07

^a Reference 4.

^b This prediction is based on the assumption that the $T = 3$ state in ^{38}Sc lies at the same excitation as its analog in ^{38}Cl .

²⁵ These calculations use a harmonic-oscillator wave function to describe the transferred nucleons; at some suitably large radius this is matched to a Hankel function which corresponds to the total observed separation energy. To test the sensitivity of the results to the nature of this form factor, the calculations were repeated using Woods-Saxon wave functions where the binding energy of each nucleon was taken to be one-half the observed separation energy. Essentially the same results were obtained.

²⁶ I. S. Towner and J. C. Hardy, *Advan. Phys.* **18**, 401 (1969).

²³ R. N. Glover (private communication).

²⁴ S. W. Cospers, H. Brunnader, J. Cerny, and R. L. McGrath, *Phys. Letters* **25B**, 324 (1967).

entage of both the ground and analog states are reasonably simple even if the wave functions themselves are not. This indication is similar to the more definite results recently obtained³ for certain states in the same mass region with $T_f = T_i$.

It is also of interest to investigate why no other states with $T = T_z + 2$ are produced with observable strength. The case of $^{42}\text{Ca}(p, t)^{40}\text{Ca}$ will be illustrative. The first excited $T = 2$ state in ^{40}Ca would be the 2^+ analog to the 1.46-MeV state in ^{40}Ar . If its wave function were comprised only of the term $[(1d_{3/2})_{21}^{-2}(1f_{7/2})_{01}^2]_{22}$, then DWBA calculations similar to those summarized in Table IV indicate that its intensity would be comparable to the 0^+ , $T = 2$ state. However, unlike the latter state, its configuration should not be dominated by a single term, and most other contributing terms—such as $[(1d_{3/2})_{01}^{-2}(1f_{7/2})_{21}^2]_{22}$ —have no spectroscopic strength for production from the simple target wave function. Evidently, this results in a significant reduction of the intensity with which the state is produced in the (p, t) reaction. Similar arguments apply to other $T = 2$ states in ^{40}Ca as well as to excited analog states in all the nuclei investigated.

Using the IMME [Eq. (1)] and measured energies from Table II, masses can be predicted for a number of neutron-deficient nuclei which are as yet unobserved. The results are given in Table V together with the predictions of Kelson and Garvey.⁴ Both sets of predictions agree throughout.

The method followed in this experiment has been used previously by us to identify analog states with $T \leq 2$ (where $T > |T_z|$). It has been restricted to these low values of T by the fact that the ratio in Eq. (2) is inversely proportional to $(2T_f - 1)$, and for analog states with higher values of T it was anticipated that the (p, t) cross section could be prohibitively small. The observation and firm identification of $T = 3$ states in mass 38 indicate that higher-isospin states can in fact be adequately studied. Consequently, it appears that such investigations as these can be extended to heavier nuclei, particularly those in the $(1f_{7/2})$ shell.

ACKNOWLEDGMENT

One of us (J. C. H.) gratefully acknowledges a fellowship from the Miller Institute for Basic Research in Science.

Inelastic Scattering of 42-MeV Alpha Particles by $^{25}\text{Mg}^\dagger$

J. S. BLAIR* AND I. M. NAQIB†

Department of Physics, University of Washington, Seattle, Washington 98105

(Received 27 August 1969)

Cross sections have been measured for elastic and inelastic scattering of 42-MeV α particles by ^{25}Mg in the range $\theta(\text{lab}) = 10^\circ - 60^\circ$. Six inelastic α groups were identified at the following measured $-Q$ values: 1.59, 1.94, 2.55, 2.75 (doublet), 3.400 (doublet), and 4.05 MeV. The cross sections are analyzed in terms of the distorted-wave Born-approximation version of the extended optical model and the smoothed Fraunhofer inelastic diffraction model. A general discussion is given of the transition strengths of odd-mass nuclei within the context of the strong-coupling rotational model or modifications thereof, and application is made to the present results. The main conclusions are: Inelastic scattering within the ground-state band supports the rotational model in its simplest form. Comparison of the elastic cross sections from ^{24}Mg , ^{25}Mg , and ^{26}Mg indicates the presence of a quadrupole contribution to the elastic cross section from ^{25}Mg , consistent with the strong-coupling prediction. The $\lambda = 2$ single-nucleon contribution to transitions into the lowest $K = \frac{1}{2}^+$ band appears to be very small. The excitation corresponding to the known level at 4.057 MeV suggests that this level arises from coupling a γ vibration to the ground-state band. The second $K = \frac{1}{2}^+$ band may have the same origin, although other evidence indicates that there is at least a sizable admixture of a single-nucleon orbital to this band.

I. INTRODUCTION

THE present paper is the second in a series concerned with the elastic and inelastic scattering of 42-MeV α particles from isotopes which lie in the

middle of the s - d shell. The motivation for the experiments, the general experimental procedures, and methods of theoretical analysis have already been presented in the paper¹ discussing scattering from ^{24}Mg ; only those experimental and theoretical points not already discussed that are pertinent to the nucleus ^{25}Mg will be discussed in Secs. II and III. The angular distributions, their analysis, and interpretations are presented in Sec. IV.

† Work supported in part by the U.S. Atomic Energy Commission.

* On leave 1968–69 at Department of Physics, University of Surrey, Guildford, England.

† Present address: Department of Physics, University of Kuwait, Kuwait.

¹I. M. Naqib and J. S. Blair, *Phys. Rev.* **165**, 1250 (1968).